

Measurement of long-range angular correlation and quadrupole anisotropy of pions and (anti)protons in central $d+Au$ collisions at $\sqrt{s_{NN}} = 200$ GeV

A. Adare,¹³ C. Aidala,^{38,42,43} N.N. Ajitanand,⁶⁰ Y. Akiba,^{55,56} R. Akimoto,¹² H. Al-Bataineh,⁴⁹ H. Al-Ta'ani,⁴⁹ J. Alexander,⁶⁰ K.R. Andrews,¹ A. Angerami,¹⁴ K. Aoki,^{34,55} N. Apadula,⁶¹ E. Appelt,⁶⁵ Y. Aramaki,^{12,55} R. Armendariz,⁸ E.C. Aschenauer,⁷ E.T. Atomssa,³⁵ R. Averbeck,⁶¹ T.C. Awes,⁵¹ B. Azmoun,⁷ V. Babintsev,²⁴ M. Bai,⁶ G. Baksay,¹⁹ L. Baksay,¹⁹ B. Bannier,⁶¹ K.N. Barish,⁸ B. Bassalleck,⁴⁸ A.T. Basye,¹ S. Bathe,^{5,8,56} V. Baublis,⁵⁴ C. Baumann,⁴⁴ A. Bazilevsky,⁷ S. Belikov,^{7,*} R. Belmont,⁶⁵ J. Ben-Benjamin,⁴⁵ R. Bennett,⁶¹ J.H. Bhom,⁶⁹ D.S. Blau,³³ J.S. Bok,⁶⁹ K. Boyle,^{56,61} M.L. Brooks,³⁸ D. Broxmeyer,⁴⁵ H. Buesching,⁷ V. Bumazhnov,²⁴ G. Bunce,^{7,56} S. Butsyk,³⁸ S. Campbell,⁶¹ A. Caringi,⁴⁵ P. Castera,⁶¹ C.-H. Chen,⁶¹ C.Y. Chi,¹⁴ M. Chiu,⁷ I.J. Choi,^{25,69} J.B. Choi,¹⁰ R.K. Choudhury,⁴ P. Christiansen,⁴⁰ T. Chujo,⁶⁴ P. Chung,⁶⁰ O. Chvala,⁸ V. Cianciolo,⁵¹ Z. Citron,⁶¹ B.A. Cole,¹⁴ Z. Conesa del Valle,³⁵ M. Connors,⁶¹ M. Csanád,¹⁷ T. Csörgő,⁶⁸ T. Dahms,⁶¹ S. Dairaku,^{34,55} I. Danchev,⁶⁵ K. Das,²⁰ A. Datta,⁴² G. David,⁷ M.K. Dayananda,²¹ A. Denisov,²⁴ A. Deshpande,^{56,61} E.J. Desmond,⁷ K.V. Dharmawardane,⁴⁹ O. Dietzsch,⁵⁸ A. Dion,^{28,61} M. Donadelli,⁵⁸ O. Drapier,³⁵ A. Drees,⁶¹ K.A. Drees,⁶ J.M. Durham,^{38,61} A. Durum,²⁴ D. Dutta,⁴ L. D'Orazio,⁴¹ S. Edwards,²⁰ Y.V. Efremenko,⁵¹ F. Ellinghaus,¹³ T. Engelmore,¹⁴ A. Enokizono,⁵¹ H. En'yo,^{55,56} S. Esumi,⁶⁴ B. Fadem,⁴⁵ D.E. Fields,⁴⁸ M. Finger,⁹ M. Finger, Jr.,⁹ F. Fleuret,³⁵ S.L. Fokin,³³ Z. Fraenkel,^{67,*} J.E. Frantz,^{50,61} A. Franz,⁷ A.D. Frawley,²⁰ K. Fujiwara,⁵⁵ Y. Fukao,⁵⁵ T. Fusayasu,⁴⁷ C. Gal,⁶¹ I. Garishvili,⁶² A. Glenn,³⁷ H. Gong,⁶¹ X. Gong,⁶⁰ M. Gonin,³⁵ Y. Goto,^{55,56} R. Granier de Cassagnac,³⁵ N. Grau,^{2,14} S.V. Greene,⁶⁵ G. Grim,³⁸ M. Grosse Perdekamp,²⁵ T. Gunji,¹² L. Guo,³⁸ H.-Å. Gustafsson,^{40,*} J.S. Haggerty,⁷ K.I. Hahn,¹⁸ H. Hamagaki,¹² J. Hamblen,⁶² R. Han,⁵³ J. Hanks,¹⁴ C. Harper,⁴⁵ K. Hashimoto,^{55,57} E. Haslum,⁴⁰ R. Hayano,¹² X. He,²¹ M. Heffner,³⁷ T.K. Hemmick,⁶¹ T. Hester,⁸ J.C. Hill,²⁸ M. Hohlmann,¹⁹ R.S. Hollis,⁸ W. Holzmann,¹⁴ K. Homma,²³ B. Hong,³² T. Horaguchi,^{23,64} Y. Hori,¹² D. Hornback,^{51,62} S. Huang,⁶⁵ T. Ichihara,^{55,56} R. Ichimiya,⁵⁵ H. Iinuma,³¹ Y. Ikeda,⁶⁴ K. Imai,^{29,34,55} M. Inaba,⁶⁴ A. Iordanova,⁸ D. Isenhower,¹ M. Ishihara,⁵⁵ M. Issah,⁶⁵ D. Ivanishev,⁵⁴ Y. Iwanaga,²³ B.V. Jacak,⁶¹ J. Jia,^{7,60} X. Jiang,³⁸ J. Jin,¹⁴ D. John,⁶² B.M. Johnson,⁷ T. Jones,¹ K.S. Joo,⁴⁶ D. Jouan,⁵² D.S. Jumper,¹ F. Kajihara,¹² J. Kamin,⁶¹ S. Kaneti,⁶¹ B.H. Kang,²² J.H. Kang,⁶⁹ J.S. Kang,²² J. Kapustinsky,³⁸ K. Karatsu,^{34,55} M. Kasai,^{55,57} D. Kawall,^{42,56} M. Kawashima,^{55,57} A.V. Kazantsev,³³ T. Kempel,²⁸ A. Khanzadeev,⁵⁴ K.M. Kijima,²³ J. Kikuchi,⁶⁶ A. Kim,¹⁸ B.I. Kim,³² D.J. Kim,³⁰ E.-J. Kim,¹⁰ Y.-J. Kim,²⁵ Y.K. Kim,²² E. Kinney,¹³ Á. Kiss,¹⁷ E. Kistenev,⁷ D. Kleinjan,⁸ P. Kline,⁶¹ L. Kochenda,⁵⁴ B. Komkov,⁵⁴ M. Konno,⁶⁴ J. Koster,²⁵ D. Kotov,⁵⁴ A. Král,¹⁵ A. Kravitz,¹⁴ G.J. Kunde,³⁸ K. Kurita,^{55,57} M. Kurosawa,⁵⁵ Y. Kwon,⁶⁹ G.S. Kyle,⁴⁹ R. Lacey,⁶⁰ Y.S. Lai,¹⁴ J.G. Lajoie,²⁸ A. Lebedev,²⁸ D.M. Lee,³⁸ J. Lee,¹⁸ K.B. Lee,³² K.S. Lee,³² S.H. Lee,⁶¹ S.R. Lee,¹⁰ M.J. Leitch,³⁸ M.A.L. Leite,⁵⁸ X. Li,¹¹ P. Lichtenwalner,⁴⁵ P. Liebing,⁵⁶ S.H. Lim,⁶⁹ L.A. Linden Levy,¹³ T. Liška,¹⁵ H. Liu,³⁸ M.X. Liu,³⁸ B. Love,⁶⁵ D. Lynch,⁷ C.F. Maguire,⁶⁵ Y.I. Makdisi,⁶ M.D. Malik,⁴⁸ A. Manion,⁶¹ V.I. Manko,³³ E. Mannel,¹⁴ Y. Mao,^{53,55} H. Masui,⁶⁴ F. Matathias,¹⁴ M. McCumber,^{13,61} P.L. McGaughey,³⁸ D. McGlinchey,^{13,20} C. McKinney,²⁵ N. Means,⁶¹ M. Mendoza,⁸ B. Meredith,²⁵ Y. Miake,⁶⁴ T. Mibe,³¹ A.C. Mignerey,⁴¹ K. Miki,^{55,64} A. Milov,^{7,67} J.T. Mitchell,⁷ Y. Miyachi,^{55,63} A.K. Mohanty,⁴ H.J. Moon,⁴⁶ Y. Morino,¹² A. Morreale,⁸ D.P. Morrison,^{7,†} S. Motschwiller,⁴⁵ T.V. Moukhanova,³³ T. Murakami,³⁴ J. Murata,^{55,57} S. Nagamiya,^{31,55} J.L. Nagle,^{13,‡} M. Naglis,⁶⁷ M.I. Nagy,⁶⁸ I. Nakagawa,^{55,56} Y. Nakamiya,²³ K.R. Nakamura,^{34,55} T. Nakamura,⁵⁵ K. Nakano,⁵⁵ S. Nam,¹⁸ J. Newby,³⁷ M. Nguyen,⁶¹ M. Nihashi,²³ R. Nouicer,⁷ A.S. Nyanin,³³ C. Oakley,²¹ E. O'Brien,⁷ S.X. Oda,¹² C.A. Ogilvie,²⁸ M. Oka,⁶⁴ K. Okada,⁵⁶ Y. Onuki,⁵⁵ A. Oskarsson,⁴⁰ M. Ouchida,^{23,55} K. Ozawa,¹² R. Pak,⁷ V. Pantuev,^{26,61} V. Papavassiliou,⁴⁹ B.H. Park,²² I.H. Park,¹⁸ S.K. Park,³² W.J. Park,³² S.F. Pate,⁴⁹ L. Patel,²¹ H. Pei,²⁸ J.-C. Peng,²⁵ H. Pereira,¹⁶ D.Yu. Peressouko,³³ R. Petti,⁶¹ C. Pinkenburg,⁷ R.P. Pisani,⁷ M. Proissl,⁶¹ M.L. Purschke,⁷ H. Qu,²¹ J. Rak,³⁰ I. Ravinovich,⁶⁷ K.F. Read,^{51,62} S. Rembeczki,¹⁹ K. Reygers,⁴⁴ V. Riabov,⁵⁴ Y. Riabov,⁵⁴ E. Richardson,⁴¹ D. Roach,⁶⁵ G. Roche,³⁹ S.D. Rolnick,⁸ M. Rosati,²⁸ C.A. Rosen,¹³ S.S.E. Rosendahl,⁴⁰ P. Ružička,²⁷ B. Sahlmueller,^{44,61} N. Saito,³¹ T. Sakaguchi,⁷ K. Sakashita,^{55,63} V. Samsonov,⁵⁴ S. Sano,^{12,66} M. Sarsour,²¹ T. Sato,⁶⁴ M. Savastio,⁶¹ S. Sawada,³¹ K. Sedgwick,⁸ J. Seele,¹³ R. Seidl,^{25,56} R. Seto,⁸ D. Sharma,⁶⁷ I. Shein,²⁴ T.-A. Shibata,^{55,63} K. Shigaki,²³ H.H. Shim,³² M. Shimomura,⁶⁴ K. Shoji,^{34,55} P. Shukla,⁴ A. Sickles,⁷ C.L. Silva,²⁸ D. Silvermyr,⁵¹ C. Silvestre,¹⁶ K.S. Sim,³² B.K. Singh,³ C.P. Singh,³ V. Singh,³ M. Slunečka,⁹ T. Sodre,⁴⁵ R.A. Soltz,³⁷ W.E. Sondheim,³⁸ S.P. Sorensen,⁶² I.V. Sourikova,⁷ P.W. Stankus,⁵¹ E. Stenlund,⁴⁰ S.P. Stoll,⁷ T. Sugitate,²³ A. Sukhanov,⁷ J. Sun,⁶¹ J. Sziklai,⁶⁸ E.M. Takagui,⁵⁸ A. Takahara,¹²

A. Taketani,^{55,56} R. Tanabe,⁶⁴ Y. Tanaka,⁴⁷ S. Taneja,⁶¹ K. Tanida,^{34,55,56,59} M.J. Tannenbaum,⁷ S. Tarafdar,³ A. Taranenko,⁶⁰ E. Tennant,⁴⁹ H. Themann,⁶¹ D. Thomas,¹ T.L. Thomas,⁴⁸ M. Togawa,⁵⁶ A. Toia,⁶¹ L. Tomášek,²⁷ M. Tomášek,²⁷ H. Torii,²³ R.S. Towell,¹ I. Tserruya,⁶⁷ Y. Tsuchimoto,²³ K. Utsunomiya,¹² C. Vale,⁷ H. Valle,⁶⁵ H.W. van Hecke,³⁸ E. Vazquez-Zambrano,¹⁴ A. Veicht,^{14,25} J. Velkovska,⁶⁵ R. Vértesi,⁶⁸ M. Virius,¹⁵ A. Vossen,²⁵ V. Vrba,²⁷ E. Vznuzdaev,⁵⁴ X.R. Wang,⁴⁹ D. Watanabe,²³ K. Watanabe,⁶⁴ Y. Watanabe,^{55,56} Y.S. Watanabe,¹² F. Wei,²⁸ R. Wei,⁶⁰ J. Wessels,⁴⁴ S.N. White,⁷ D. Winter,¹⁴ C.L. Woody,⁷ R.M. Wright,¹ M. Wysocki,¹³ Y.L. Yamaguchi,^{12,55} K. Yamaura,²³ R. Yang,²⁵ A. Yanovich,²⁴ J. Ying,²¹ S. Yokkaichi,^{55,56} J.S. Yoo,¹⁸ Z. You,^{38,53} G.R. Young,⁵¹ I. Younus,^{36,48} I.E. Yushmanov,³³ W.A. Zajc,¹⁴ A. Zelenski,⁶ and S. Zhou¹¹

(PHENIX Collaboration)

¹Abilene Christian University, Abilene, Texas 79699, USA

²Department of Physics, Augustana College, Sioux Falls, South Dakota 57197, USA

³Department of Physics, Banaras Hindu University, Varanasi 221005, India

⁴Bhabha Atomic Research Centre, Bombay 400 085, India

⁵Baruch College, City University of New York, New York, New York, 10010 USA

⁶Collider-Accelerator Department, Brookhaven National Laboratory, Upton, New York 11973-5000, USA

⁷Physics Department, Brookhaven National Laboratory, Upton, New York 11973-5000, USA

⁸University of California - Riverside, Riverside, California 92521, USA

⁹Charles University, Ovocný trh 5, Praha 1, 116 36, Prague, Czech Republic

¹⁰Chonbuk National University, Jeonju, 561-756, Korea

¹¹Science and Technology on Nuclear Data Laboratory, China Institute of Atomic Energy, Beijing 102413, P. R. China

¹²Center for Nuclear Study, Graduate School of Science, University of Tokyo, 7-3-1 Hongo, Bunkyo, Tokyo 113-0033, Japan

¹³University of Colorado, Boulder, Colorado 80309, USA

¹⁴Columbia University, New York, New York 10027 and Nevis Laboratories, Irvington, New York 10533, USA

¹⁵Czech Technical University, Zikova 4, 166 36 Prague 6, Czech Republic

¹⁶Dapnia, CEA Saclay, F-91191, Gif-sur-Yvette, France

¹⁷ELTE, Eötvös Loránd University, H - 1117 Budapest, Pázmány P. s. 1/A, Hungary

¹⁸Ewha Womans University, Seoul 120-750, Korea

¹⁹Florida Institute of Technology, Melbourne, Florida 32901, USA

²⁰Florida State University, Tallahassee, Florida 32306, USA

²¹Georgia State University, Atlanta, Georgia 30303, USA

²²Hanyang University, Seoul 133-792, Korea

²³Hiroshima University, Kagamiyama, Higashi-Hiroshima 739-8526, Japan

²⁴IHEP Protvino, State Research Center of Russian Federation, Institute for High Energy Physics, Protvino, 142281, Russia

²⁵University of Illinois at Urbana-Champaign, Urbana, Illinois 61801, USA

²⁶Institute for Nuclear Research of the Russian Academy of Sciences, prospekt 60%-letiya Oktyabrya 7a, Moscow 117312, Russia

²⁷Institute of Physics, Academy of Sciences of the Czech Republic, Na Slovance 2, 182 21 Prague 8, Czech Republic

²⁸Iowa State University, Ames, Iowa 50011, USA

²⁹Advanced Science Research Center, Japan Atomic Energy Agency, 2-4

Shirakata Shirane, Tokai-mura, Naka-gun, Ibaraki-ken 319-1195, Japan

³⁰Helsinki Institute of Physics and University of Jyväskylä, P.O.Box 35, FI-40014 Jyväskylä, Finland

³¹KEK, High Energy Accelerator Research Organization, Tsukuba, Ibaraki 305-0801, Japan

³²Korea University, Seoul, 136-701, Korea

³³Russian Research Center "Kurchatov Institute", Moscow, 123098 Russia

³⁴Kyoto University, Kyoto 606-8502, Japan

³⁵Laboratoire Leprince-Ringuet, Ecole Polytechnique, CNRS-IN2P3, Route de Saclay, F-91128, Palaiseau, France

³⁶Physics Department, Lahore University of Management Sciences, Lahore, Pakistan

³⁷Lawrence Livermore National Laboratory, Livermore, California 94550, USA

³⁸Los Alamos National Laboratory, Los Alamos, New Mexico 87545, USA

³⁹LPC, Université Blaise Pascal, CNRS-IN2P3, Clermont-Fd, 63177 Aubiere Cedex, France

⁴⁰Department of Physics, Lund University, Box 118, SE-221 00 Lund, Sweden

⁴¹University of Maryland, College Park, Maryland 20742, USA

⁴²Department of Physics, University of Massachusetts, Amherst, Massachusetts 01003-9337, USA

⁴³Department of Physics, University of Michigan, Ann Arbor, Michigan 48109-1040, USA

⁴⁴Institut für Kernphysik, University of Muenster, D-48149 Muenster, Germany

⁴⁵Muhlenberg College, Allentown, Pennsylvania 18104-5586, USA

⁴⁶Myongji University, Yongin, Kyonggido 449-728, Korea

⁴⁷Nagasaki Institute of Applied Science, Nagasaki-shi, Nagasaki 851-0193, Japan

⁴⁸University of New Mexico, Albuquerque, New Mexico 87131, USA

⁴⁹New Mexico State University, Las Cruces, New Mexico 88003, USA

⁵⁰Department of Physics and Astronomy, Ohio University, Athens, Ohio 45701, USA

⁵¹Oak Ridge National Laboratory, Oak Ridge, Tennessee 37831, USA

⁵²IPN-Orsay, Universite Paris Sud, CNRS-IN2P3, BP1, F-91406, Orsay, France

⁵³Peking University, Beijing 100871, P. R. China

⁵⁴PNPI, Petersburg Nuclear Physics Institute, Gatchina, Leningrad region, 188300, Russia

⁵⁵RIKEN Nishina Center for Accelerator-Based Science, Wako, Saitama 351-0198, Japan

⁵⁶RIKEN BNL Research Center, Brookhaven National Laboratory, Upton, New York 11973-5000, USA

⁵⁷Physics Department, Rikkyo University, 3-34-1 Nishi-Ikebukuro, Toshima, Tokyo 171-8501, Japan

⁵⁸Universidade de São Paulo, Instituto de Física, Caixa Postal 66318, São Paulo CEP05315-970, Brazil

⁵⁹Seoul National University, Seoul, Korea

⁶⁰Chemistry Department, Stony Brook University, SUNY, Stony Brook, New York 11794-3400, USA

⁶¹Department of Physics and Astronomy, Stony Brook University, SUNY, Stony Brook, New York 11794-3800, USA

⁶²University of Tennessee, Knoxville, Tennessee 37996, USA

⁶³Department of Physics, Tokyo Institute of Technology, Oh-okayama, Meguro, Tokyo 152-8551, Japan

⁶⁴Institute of Physics, University of Tsukuba, Tsukuba, Ibaraki 305, Japan

⁶⁵Vanderbilt University, Nashville, Tennessee 37235, USA

⁶⁶Waseda University, Advanced Research Institute for Science and

Engineering, 17 Kikui-cho, Shinjuku-ku, Tokyo 162-0044, Japan

⁶⁷Weizmann Institute, Rehovot 76100, Israel

⁶⁸Institute for Particle and Nuclear Physics, Wigner Research Centre for Physics, Hungarian Academy of Sciences (Wigner RCP, RMKI) H-1525 Budapest 114, POBox 49, Budapest, Hungary

⁶⁹Yonsei University, IPAP, Seoul 120-749, Korea

(Dated: December 18, 2021)

We present azimuthal angular correlations between charged hadrons and energy deposited in calorimeter towers in central d +Au and minimum bias p + p collisions at $\sqrt{s_{NN}} = 200$ GeV. The charged hadron is measured at midrapidity $|\eta| < 0.35$, and the energy is measured at large rapidity ($-3.7 < \eta < -3.1$, Au-going direction). An enhanced near-side angular correlation across $|\Delta\eta| > 2.75$ is observed in d +Au collisions. Using the event plane method applied to the Au-going energy distribution, we extract the anisotropy strength v_2 for inclusive charged hadrons at midrapidity up to $p_T = 4.5$ GeV/ c . We also present the measurement of v_2 for identified π^\pm and (anti)protons in central d +Au collisions, and observe a mass-ordering pattern similar to that seen in heavy ion collisions. These results are compared with viscous hydrodynamic calculations and measurements from p +Pb at $\sqrt{s_{NN}} = 5.02$ TeV. The magnitude of the mass-ordering in d +Au is found to be smaller than that in p +Pb collisions, which may indicate smaller radial flow in lower energy d +Au collisions.

PACS numbers: 25.75.Dw

Asymmetric nuclear collisions, d +Au and p +Pb, have been studied at the Relativistic Heavy Ion Collider (RHIC) and the Large Hadron Collider (LHC) to understand baseline nuclear effects for heavy-ion collisions in which hot nuclear matter is made. The d +Au and p +Pb systems have generally been considered too small to create significant quantities of hot nuclear matter. This assumption has been challenged in p +Pb at $\sqrt{s_{NN}} = 5.02$ TeV with the measurements of (i) near-side azimuthal angular correlations across a large pseudorapidity gap [1–3] and (ii) the anisotropy parameters v_n ($n=2,3$), which are used to quantify the amplitude of the particle azimuthal distribution with respect to the reaction-plane (Ψ_{RP}) as $dN/d(\phi - \Psi_{RP}) \propto 1 + 2 \sum_{n=1}^{\infty} v_n \cos(n(\phi - \Psi_{RP}))$ [4, 5]. A sizable v_2 has also been observed in d +Au at $\sqrt{s_{NN}} = 200$ GeV, albeit with large uncertainties, from measurement of hadron pair correlations in a limited rapidity range ($0.7 > |\Delta\eta| > 0.48$) [6].

At the LHC and at RHIC, hydrodynamic models successfully reproduce data from both heavy ion and p / d +nucleus collisions, under the assumption that the azimuthal angular correlations arise primarily in the evo-

lution of a created fluid medium [7–9]. In the Color Glass Condensate model, near-side correlations across large rapidity arise due to enhanced gluon emission from “glasma” diagrams at high parton densities [10–12]. If hydrodynamics is the primary cause of the observed effects then there should be a mass-ordering of the magnitudes of v_2 for identified particles, in which heavier particles show smaller v_2 values at low $p_T < 1.5$ GeV/ c [13, 14]. Recently, this mass-ordering has been observed in p +Pb collisions at LHC for v_2 of π^\pm and p, \bar{p} [15].

Long-range angular correlations and elliptic anisotropy of inclusive and identified hadrons in p + p and d +Au collisions at RHIC can provide crucial test as to whether a hydrodynamically expanding medium is created in these small systems. In this Letter, we report measurements of azimuthal correlations in top 5% central d +Au and minimum bias p + p collisions between charged hadrons at midrapidity ($|\eta| < 0.35$) and energy deposited at large rapidity $-3.7 < \eta < -3.1$ (Au-going direction). We also report v_2 for inclusive hadron and identified pions and (anti)protons in d +Au at midrapidity using an event plane across $|\Delta\eta| > 2.75$.

The data were obtained from $p+p$ in the 2008 and 2009 experimental runs and $d+Au$ in the 2008 run with the PHENIX detector. The event centrality class in $d+Au$ collisions is determined as a percentile of the total charge measured in the PHENIX beam-beam counter covering $-3.9 < \eta < -3.0$ on the Au-going side [16]. For the top 5% central $d+Au$ collisions, the corresponding number of binary collisions and number of participants are 18.1 ± 1.2 and 17.8 ± 1.2 respectively [16].

Charged particles used in this analysis are reconstructed in the two PHENIX central-arm tracking systems, consisting of drift chambers and multi-wire proportional pad chambers (PC) [17]. Each arm covers $\pi/2$ in azimuth and $|\eta| < 0.35$, and the tracking system achieves a momentum resolution of $0.7\% \oplus 1.1\% p$ GeV/ c .

The drift-chamber tracks are matched to hits in the third layer of the PC, reducing the contribution of tracks originating from decays and photon conversions. Hadron identification is achieved using the time-of-flight detectors, with different technologies in the east and west arms, for which the timing resolutions are 130 ps and 95 ps, respectively. Pions and (anti)proton tracks are identified with over 99% purity at momenta up to 3 GeV/ c [18, 19] in both systems.

Energy deposited at large rapidity in the Au-going direction is measured by the towers in the south-side Muon Piston Calorimeter (MPC-S) [20]. The MPC-S comprises 192 towers of PbWO₄ crystal covering 2π in azimuth and $-3.7 < \eta < -3.1$ in pseudorapidity, with each tower subtending approximately $\delta\eta \times \delta\phi \approx 0.12 \times 0.18$. Over 95% of the energy detected in the MPC is from photons, which are primarily produced in the decays of π^0 and η mesons. Photons are well localized, as each will deposit over 90% of its energy into one tower if it hits the tower's center. To avoid the background from noncollision noise sources and cut out the deposits by minimum ionization particles (~ 245 MeV), we select towers with deposited energy $E_{\text{Tower}} > 3$ GeV.

We first examine the long-range azimuthal angular correlation of pairs consisting of one track in the central arm and one tower in the MPC-S. Because the towers are mainly fired by photons, and the azimuthal extent of each energy deposition is much smaller than the size of azimuthal angular correlation from jet or elliptic flow, these track-tower pair correlations will be good proxies for hadron-photon correlations without attempting to reconstruct individual photon showers. We construct the signal distribution $S(\Delta\phi, p_T)$ of track-tower pairs over relative azimuthal opening angle $\Delta\phi \equiv \phi_{\text{Track}} - \phi_{\text{Tower}}$, each with weight w_{tower} , in bins of track transverse momentum p_T .

$$S(\Delta\phi, p_T) = \frac{d(w_{\text{Tower}} N_{\text{Same event}}^{\text{Track}(p_T) - \text{Tower}})}{d\Delta\phi} \quad (1)$$

Here ϕ_{Track} is the azimuth of the track as it leaves the

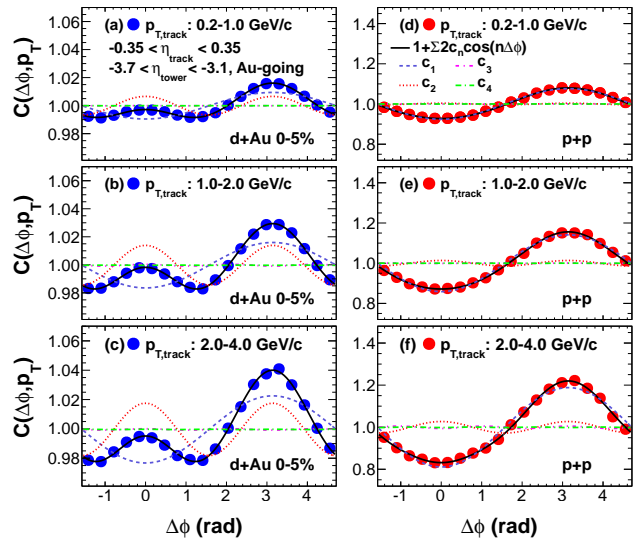


FIG. 1: The azimuthal correlation functions $C(\Delta\phi, p_T)$, as defined in Eq. 2, for track-tower pairs with different track p_T selections in 0%–5% central $d+Au$ collisions (left) and minimum bias $p+p$ collisions (right) at $\sqrt{s_{NN}} = 200$ GeV. From top to bottom, the track p_T bins are 0.2–1.0 GeV/ c , 1.0%–2.0 GeV/ c and 2.0%–4.0 GeV/ c . The pairs are formed between charged tracks measured in the PHENIX central arms at $|\eta| < 0.35$ and towers in the MPC-S calorimeter ($-3.7 < \eta < -3.1$, Au-going). A near-side peak is observed in the central $d+Au$ which is not seen in minimum bias $p+p$. Each correlation function is fit with a four-term Fourier cosine expansion; the individual components $n = 1$ to $n = 4$ are drawn on each panel, together with the fit function sum.

primary vertex, ϕ_{Tower} is the azimuth of the center of the calorimeter tower. The w_{Tower} is chosen as the tower's transverse energy $E_T = E_{\text{Tower}} \sin(\theta_{\text{Tower}})$. This quantity is found to be less sensitive to occupancy effects which result from multiple hits in the same tower, or a single hit which distributes its signal between more than one tower. To correct for the nonuniform PHENIX azimuthal acceptance in the central arm tracking system, we then construct the corresponding “mixed-event” distribution $M(\Delta\phi, p_T)$ over track-tower pairs, where the tracks and tower signals are from different events in the same centrality and vertex position class. We then construct the normalized correlation function

$$C(\Delta\phi, p_T) = \frac{S(\Delta\phi, p_T)}{M(\Delta\phi, p_T)} \frac{\int_0^{2\pi} M(\Delta\phi, p_T) d\Delta\phi}{\int_0^{2\pi} S(\Delta\phi, p_T) d\Delta\phi} \quad (2)$$

whose shape is proportional to the true pairs distribution over $\Delta\phi$.

Figure 1 shows the correlation functions $C(\Delta\phi, p_T)$ for different p_T bins, for the top 5% most central $d+Au$ collisions and for minimum bias $p+p$ collisions. Near head-on $d+Au$ collisions show a visible enhancement of

near-side pairs, producing a local maximum in the distribution at $\Delta\phi \sim 0$, which is not seen in the $p+p$ data. We analyze the distributions by fitting each $C(\Delta\phi, p_T)$ to a four-term Fourier cosine expansion, $f(\Delta\phi) = 1 + \sum_{n=1}^4 c_n(p_T) \cos(n\Delta\phi)$; the sum function and each individual cosine component are plotted in Fig. 1 for each distribution. We observe that the $p+p$ distribution shape is described almost entirely by the dipole term $\cos(\Delta\phi)$, which could be the product of dijet fragmentation or other transverse-momentum-conserving processes; while the shape in central $d+Au$ exhibits both dipole and quadrupole $\cos(2\Delta\phi)$ terms with similar magnitudes. Both c_3 and c_4 are found to be ≈ 0 , as shown in Fig. 1.

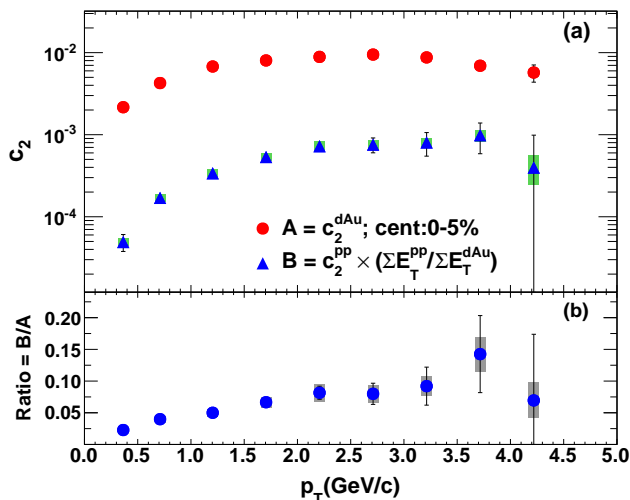


FIG. 2: Panel (a) shows $c_2(p_T)$ for track-tower pairs from 0%–5% $d+Au$ collisions and $c_2(p_T)$ for pairs in minimum bias $p+p$ collisions times the dilution factor ($\sum E_T^{pp}/\sum E_T^{dAu}$). Panel (b) shows their ratio, indicating that the contribution to the c_2 amplitude in $d+Au$ from elementary processes present in $p+p$ are small, only a few percent at low p_T and rising to only 10% by 4.5 GeV/c. Both statistical (bar) and systematic (band) uncertainties are shown.

Figure 2 shows the fitted c_2 parameters from the $d+Au$ and $p+p$ with both statistical and systematic uncertainties. We estimate contributions to systematic uncertainties from three main sources: (1) tracking backgrounds from weak decays and photon conversions, (2) noise in MPC towers, (3) multiple collisions in a bunch crossing (pile-up) in $d+Au$ collisions. We estimate the tracking background contribution by reducing the spatial matching windows in the third layer of the PC from 3σ to 2σ , and find that the change is less than 2% fractionally in c_2 . To estimate the contribution of noise backgrounds in the MPC towers we vary the tower threshold for minimum deposited energy from 3 GeV to 0.3 GeV, and find a resulting difference of less than 5%. To study the pile-up effect in $d+Au$ collisions we separate the $d+Au$ data set into two groups, one from a period with lower lu-

minosity and the other with the higher luminosity. The corresponding pile-up fractions in central $d+Au$ are 3.5% and 7.0%, respectively. The c_2^{dAu} in the lower luminosity data set is around 5% higher than that in higher luminosity for $p_T < 2$ GeV/c and increases to 10% for $p_T > 2$ GeV/c. Additionally, we compare c_2^{pp} results for $p+p$ data taken in the 2008 and 2009 running periods, and see a difference of less than 5% for $p_T < 1$ GeV/c, increasing to 15% for $p_T > 3$ GeV/c.

Some portion of the correlation quadrupole strength c_2 in the $d+Au$ data could be due to elementary processes such as dijet fragmentation and resonance decays. We can estimate the effect of such processes under the assumptions that (i) all correlations present in minimum bias $p+p$ collisions are due to elementary processes, and (ii) those same processes occur, unmodified, within $N+N$ collisions in the $d+Au$ system. In this case, we would expect the contribution from elementary processes to be equal to the $c_2^{pp}(p_T)$ but diluted by the increase in particle multiplicity between $p+p$ and $d+Au$ (see also the “scalar product method”, as in [21, 22]). We estimate the ratio of the $p+p$ to $d+Au$ general multiplicities by measuring the ratio of the total transverse energy $\sum E_T$ seen in the MPC-S calorimeter in $p+p$ versus $d+Au$ events, which we find to be approximately $1/(17.9 \pm 0.35)$. We can then separate $c_2^{dAu}(p_T)$ into elementary and nonelementary components:

$$\begin{aligned} c_2^{dAu}(p_T) &= c_2^{\text{Non-elem.}}(p_T) + c_2^{\text{Elem.}}(p_T) \\ &\approx c_2^{\text{Non-elem.}}(p_T) + c_2^{pp}(p_T) \frac{\sum E_T^{pp}}{\sum E_T^{dAu}} \quad (3) \end{aligned}$$

The ratio in Fig. 2(b) shows that the contribution to c_2^{dAu} from elementary processes is indeed small, ranging from a few percent at the lowest p_T to around 10% at the highest p_T . The presence of the near-side peak in the pairs distribution, and the corresponding quadrupole term in the cosine expansion indicate some physics process in the central $d+Au$ system that is not present in minimum bias $p+p$ collisions, creating an additional source of correlations across rapidity in these collisions. The formation of a medium that evolves hydrodynamically is one such possibility [7–9], but processes such as initial state gluon saturation [11, 12] could also create such an effect.

We analyze this additional correlation by reconstructing the v_2 of charged hadrons, pions, and (anti)protons at midrapidity with the standard event plane method [23]. The v_2 is measured as $v_2(p_T) = \langle \cos 2(\phi^{\text{Particle}} - \Psi_2^{\text{Obs}}) \rangle / \text{Res}(\Psi_2^{\text{Obs}})$, where the average is over particles in the p_T bin and over events. The second order event plane direction Ψ_2^{Obs} is determined using the MPC-S (Au-going). The study of correlation strength as above indicates that the elementary-process contribution to the event plane v_2 result is similarly small, less than 10% fractionally out to $p_T = 4.5$ GeV/c. The event plane

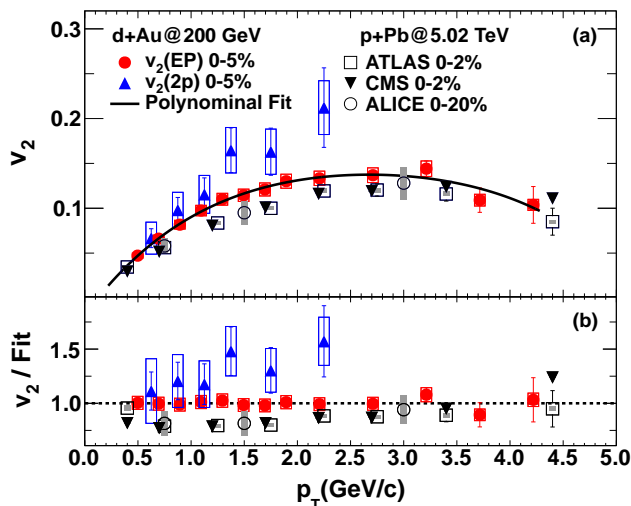


FIG. 3: Measured $v_2(EP)$ for midrapidity charged tracks in 0%–5% central $d+Au$ at $\sqrt{s_{NN}} = 200$ GeV using the event plane method in Panel (a). Also shown are v_2 measured in central $p+Pb$ collisions at $\sqrt{s_{NN}} = 5.02$ TeV [2, 3, 5], and our prior measurements with two particle correlations ($v_2(2p)$) for $d+Au$ collisions [6]. A polynomial fit to the current measurement and the ratios of experimental values to the fit are shown in the panel (b).

resolution $\text{Res}(\Psi_2^{\text{Obs}})$ is calculated through the standard three subevents method [23, 24], with the other two event planes being (i) the second order event plane determined from central-arm tracks, restricted to low p_T ($0.2 \text{ GeV}/c < p_T < 2.0 \text{ GeV}/c$) to minimize contribution from jet fragments; and (ii) the first order event plane measured with spectator neutrons in the shower-maximum detector on the Au-going side ($\eta < -6.5$) [24, 25]. The systematic uncertainties on the v_2 of charged hadrons are mainly from the tracking background and pile-up effects, as described above, and also from the difference in v_2 from different event plane determinations. To estimate the systematic uncertainty of the latter we compare the v_2 extracted with the MPC-S event plane with that using the south (Au-going) beam-beam counter, and the two measurements of v_2 are consistent to within 5%.

The v_2 of charged hadrons for 0%–5% central $d+Au$ events with event plane methods are shown in Fig. 3(a) as $v_2(EP)$ for p_T up to 4.5 GeV/c , along with a polynomial fit through the points. Also shown are our earlier measurement with two particle correlations ($v_2(2p)$) and the v_2 measured in the central $p+Pb$ collisions at LHC. Figure 3(b) shows the ratios of all of these measurements divided by the fitting results. The v_2 from our prior measurements exceed the current measurement; differences range from about 15% at $p_T = 1.0 \text{ GeV}/c$ and increases to about 50% at $p_T = 2.2 \text{ GeV}/c$. However, the differences are within the stated uncertainties from prior measurements.

The present v_2 measurement is closer to that of $p+Pb$

collisions [2, 3, 5], with much improved uncertainties and extended p_T range. It is about 20% higher than that of $p+Pb$ at $p_T = 1 \text{ GeV}/c$, and the difference decreases to few percent at $p_T > 2.0 \text{ GeV}/c$.

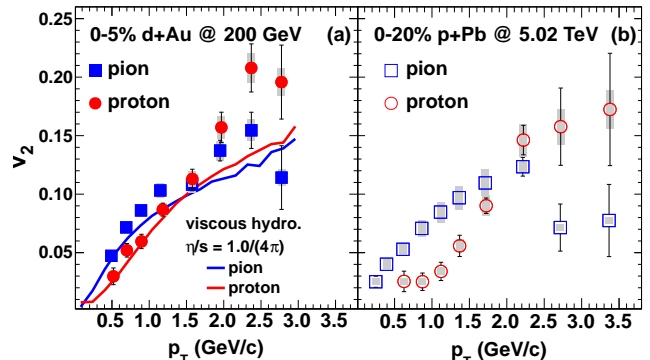


FIG. 4: Measured $v_2(p_T)$ for identified pions and (anti)protons, each charged combined, in 0%–5% central $d+Au$ collisions at RHIC. In panel (a) the data are compared with the calculation from a viscous hydrodynamic model [26–28], and in panel (b) the v_2 data for pions and protons in 0%–20% central $p+Pb$ collisions at LHC are shown for comparison [15].

Figure 4 shows the midrapidity $v_2(p_T)$ for identified charged pions and (anti)protons, with charge signs combined for each species, up to $p_T = 3 \text{ GeV}/c$ using the event plane method; the systematic uncertainties are the same as for inclusive charged hadrons. A distinctive mass-splitting can be seen. The meson v_2 is higher than the baryon for $p_T < 1.5 \text{ GeV}/c$, as has been seen universally in heavy-ion collisions at RHIC [29–34]. Figure 4(a) also shows calculations with Glauber initial conditions for viscous hydrodynamics starting at $\tau = 0.5 \text{ fm}/c$ with $\eta/s = 1.0/(4\pi)$, followed by a hadronic cascade [26–28]. The splitting at lower p_T is also seen in the calculation. Because there are no known CGC calculations available that would indicate a mass-splitting, it may be challenging – even in principle – to establish the observed mass dependence in the initial stages of the collision. The identified particle v_2 in 0%–20% $p+Pb$ collisions are shown in Fig. 4(b) for comparison [15]. The magnitude of the mass-splitting in RHIC $d+Au$ is smaller than that seen in LHC $p+Pb$, which could be an indicator of stronger radial flow in the higher energy collisions.

We have presented measurements of long-range azimuthal correlations between particles at midrapidity and at backward rapidity (Au-going direction) in 0%–5% central $d+Au$ collisions at $\sqrt{s_{NN}} = 200$ GeV. We find a near-side azimuthal angular correlation in these collisions for pairs across $|\Delta\eta| > 2.75$ which is not apparent in minimum bias $p+p$ collisions at the same collision energy. The anisotropy strength v_2 is measured for midrapidity particles with respect to a global event plane determined from a region separated by the same pseudorapidity in-

terval. The v_2 values measured with these long-range event plane correlations are qualitatively similar to those observed in central p +Pb collisions at $\sqrt{s_{NN}} = 5.02$ TeV. Further evidence for the applicability of hydrodynamics in these collisions is seen in the observed mass ordering of v_2 for identified pions and (anti)protons at midrapidity. This ordering can be described by a viscous hydrodynamic model, where they are believed to reflect radial flow in hydrodynamics. The magnitude of mass-splitting in $v_2(p_t)$ is found to be smaller in d +Au collisions in comparison to p +Pb collisions at higher energies, possibly indicating smaller radial flow in d +Au at $\sqrt{s_{NN}} = 200$ GeV.

We thank the staff of the Collider-Accelerator and Physics Departments at Brookhaven National Laboratory and the staff of the other PHENIX participating institutions for their vital contributions. We acknowledge support from the Office of Nuclear Physics in the Office of Science of the Department of Energy, the National Science Foundation, Abilene Christian University Research Council, Research Foundation of SUNY, and Dean of the College of Arts and Sciences, Vanderbilt University (U.S.A), Ministry of Education, Culture, Sports, Science, and Technology and the Japan Society for the Promotion of Science (Japan), Conselho Nacional de Desenvolvimento Científico e Tecnológico and Fundação de Amparo à Pesquisa do Estado de São Paulo (Brazil), Natural Science Foundation of China (P. R. China), Ministry of Education, Youth and Sports (Czech Republic), Centre National de la Recherche Scientifique, Commissariat à l'Énergie Atomique, and Institut National de Physique Nucléaire et de Physique des Particules (France), Bundesministerium für Bildung und Forschung, Deutscher Akademischer Austausch Dienst, and Alexander von Humboldt Stiftung (Germany), Hungarian National Science Fund, OTKA (Hungary), Department of Atomic Energy and Department of Science and Technology (India), Israel Science Foundation (Israel), National Research Foundation of Korea of the Ministry of Science, ICT, and Future Planning (Korea), Physics Department, Lahore University of Management Sciences (Pakistan), Ministry of Education and Science, Russian Academy of Sciences, Federal Agency of Atomic Energy (Russia), VR and Wallenberg Foundation (Sweden), the U.S. Civilian Research and Development Foundation for the Independent States of the Former Soviet Union, the Hungarian American Enterprise Scholarship Fund, the US-Hungarian Fulbright Foundation for Educational Exchange, and the US-Israel Binational Science Foundation.

* Deceased

† PHENIX Co-Spokesperson: morrison@bnl.gov

‡ PHENIX Co-Spokesperson: jamie.nagle@colorado.edu

[1] S. Chatrchyan et al. (CMS Collaboration), Phys. Lett. B **718**, 795 (2013).

- [2] G. Aad et al. (ATLAS Collaboration), Phys. Rev. Lett. **110**, 182302 (2013).
- [3] B. Abelev et al. (ALICE Collaboration), Phys. Lett. B **719**, 29 (2013).
- [4] G. Aad et al. (ATLAS Collaboration), Phys. Lett. B **725**, 60 (2013).
- [5] S. Chatrchyan et al. (CMS Collaboration), Phys. Lett. B **724**, 213 (2013).
- [6] A. Adare et al. (PHENIX Collaboration), Phys. Rev. Lett. **111**, 212301 (2013).
- [7] P. Bozek and W. Broniowski, Phys. Rev. C **88**, 014903 (2013).
- [8] A. Bzdak, B. Schenke, P. Tribedy, and R. Venugopalan, Phys. Rev. C **87**, 064906 (2013).
- [9] G.-Y. Qin and B. Mueller, arXiv:1306.3439.
- [10] K. Dusling and R. Venugopalan, Phys. Rev. Lett. **108**, 262001 (2012).
- [11] K. Dusling and R. Venugopalan, Phys. Rev. D **87**, 054014 (2012).
- [12] K. Dusling and R. Venugopalan, Phys. Rev. D **87**, 094034 (2013).
- [13] P. Huovinen, P. Kolb, U. W. Heinz, P. Ruuskanen, and S. Voloshin, Phys. Lett. B **503**, 58 (2001).
- [14] P. Bozek, W. Broniowski, and G. Torrieri, arXiv:1307.5060.
- [15] B. B. Abelev et al. (ALICE Collaboration), Phys. Lett. B **726**, 164 (2013).
- [16] A. Adare et al. (PHENIX Collaboration), arXiv:1310.4793.
- [17] K. Adcox et al. (PHENIX Collaboration), Nucl. Instrum. Meth. A **499**, 489 (2003).
- [18] A. Adare et al. (PHENIX Collaboration), Phys. Rev. C **88**, 024906 (2013).
- [19] A. Adare et al. (PHENIX Collaboration), Phys. Rev. C **85**, 064914 (2012).
- [20] M. Chiu (PHENIX Collaboration), Amer. Inst. Phys. Conf. Proc. **915**, 539 (2007).
- [21] J. Adams et al. (STAR Collaboration), Phys. Rev. Lett. **93**, 252301 (2004).
- [22] J. Adams et al. (STAR Collaboration), Phys. Rev. C **72**, 014904 (2005).
- [23] A. M. Poskanzer and S. A. Voloshin, Phys. Rev. C **58**, 1671 (1998).
- [24] S. Afanasiev et al. (PHENIX Collaboration), Phys. Rev. C **80**, 024909 (2009).
- [25] A. J. Baltz, C. Chasman, and S. N. White, Nucl. Instr. Methods A **417**, 1 (1998).
- [26] J. Nagle et al., arXiv:1312.4565.
- [27] P. Romatschke, private communication.
- [28] M. Luzum and P. Romatschke, Phys. Rev. C **78**, 034915 (2008).
- [29] S. S. Adler et al. (PHENIX Collaboration), Phys. Rev. Lett. **91**, 182301 (2003).
- [30] J. Adams et al. (STAR Collaboration), Phys. Rev. Lett. **92**, 052302 (2004).
- [31] A. Adare et al. (PHENIX Collaboration), Phys. Rev. Lett. **98**, 162301 (2007).
- [32] S. Afanasiev et al. (PHENIX Collaboration), Phys. Rev. Lett. **99**, 052301 (2007).
- [33] B. Abelev et al. (the STAR Collaboration), Phys. Rev. C **75**, 054906 (2007).
- [34] B. Abelev et al. (STAR Collaboration), Phys. Rev. C **77**, 054901 (2008).